PHILOSOPHICAL TRANSACTIONS OF THE ROYAL SOCIETY A MATHEMATICAL, PHYSICAL & ENGINEERING SCIENCES

The Solid State Dehydration of d Lithium Potassium Tartrate Monohydrate is Completed in Two Rate Processes I. The Deceleratory Diffusion-Controlled First Reaction

Andrew K. Galwey, Genevieve M. Laverty, Nikolai A. Baranov and Vladimir B. Okhotnikov

Phil. Trans. R. Soc. Lond. A 1994 **347**, 139-156
doi: 10.1098/rsta.1994.0042

The solid state dehydration of *d* lithium potassium tartrate monohydrate is completed in two rate processes

I. The deceleratory diffusion-controlled first reaction

By Andrew K. Galwey[1], Geneviève M. Laverty[1], Nikolai A. Baranov[2] and Vladimir B. Okhotnikov[2]

[1] *School of Chemistry, The Queen's University of Belfast, Belfast BT9 5AG, U.K.*
[2] *Institute of Solid State Chemistry, Derzhavina 18, Novosibirsk 630091, Russia*

A kinetic and mechanistic study of the dehydration of *d* lithium potassium tartrate monohydrate has been undertaken. Water evolution is completed through two separate rate processes. The first reaction is the deceleratory, diffusion-controlled release of water from the superficial zones of the reactant crystals. The yield of this process corresponds to the dehydration of a superficial layer of crystal, thickness 10 μm. About 4% of the constituent water was evolved from the single crystals studied, rising to 50% from crushed powder reactants. The second reaction, reported in Part II, is a nucleation and growth process yielding the crystalline anhydrous salt.

Gravimetric measurements for the first reaction identified three distinct dehydration processes. The first step was the rapid release of loosely bonded superficial water. The subsequent two deceleratory stages are characterized as diffusive loss of H_2O molecules from a crystal zone that is at first ordered but later becomes disordered as the water-site vacancy concentration increases. Rate measurements based on water evolution measured the activation energy of this third step as 153 ± 4 kJ mol^{-1}. Irreproducibility of rate data is ascribed to variations in numbers and distributions of imperfections between individual crystals. The extent and rate of the first reaction increased when initiated in small pressures of water vapour. Electron microscope observations identified a structural discontinuity *ca.* 1 μm below reacted crystal faces, evidence of superficial retexturing of the reactant.

Rates of powder dehydrations were more reproducible than those of crystals but the kinetic behaviour was similar. The same rate equations were obeyed and the activation energy was unaltered.

Water loss during the first reaction of this crystalline hydrate gives a comprehensive layer of extensively dehydrated material across all surfaces. Subsequently, in or under this water depleted layer, salt is recrystallized and dehydration continues as a nucleation and growth reaction (part II, following paper).

1. Introduction

Studies of crystal dehydrations have contributed significantly to the development of the theory of solid state reactions (Brown *et al.* 1980). The early publications by Garner and co-workers on water losses from chrome alum (Cooper & Garner 1940) and from copper sulphate (Garner & Tanner 1930), among other crystalline hydrates

Phil. Trans. R. Soc. Lond. A (1994) **347**, 139–156
Printed in Great Britain

(Garner 1955), notably contributed to the establishment of the nucleation and growth reaction mechanism by recognizing the advancing active reaction interface as the zone of chemical change. More recent developments have considered the chemistry of these interfacial changes in greater detail and two general categories of dehydration behaviour can now be distinguished. In those solids that retain the structure of the original reactant, the rate of water evolution is usually controlled by the rate of diffusive escape from interlayer sheets, as has been described for sheet silicate minerals (Brown *et al.* 1980) and gypsum (Okhotnikov *et al.* 1987). Alternatively, many hydrates recrystallize to the product structure at or near the interface that advances into unreacted material. Some progress is being made towards the detailed characterization of such reactant/product contact zones, for example there is evidence that water is lost in advance of the nucleus periphery that is the microscopically recognizable feature of the reaction interface (Galwey *et al.* 1990; Boldyrev *et al.* 1987). In alum dehydrations it has been shown (Galwey *et al.* 1981) that, under water loss conditions, all outer crystal faces are modified, believed to be a consequence of dehydration, though the initiation of sustained reaction occurs at only a limited number of nucleation sites (Galwey & Laverty 1990) that subsequently develop as growth nuclei.

To extend understanding of the chemistry of dehydrations of crystalline hydrates, sometimes regarded as model compounds in the field of solid state chemistry, we have undertaken a kinetic and mechanistic study of the dehydration of *d* lithium potassium tartrate monohydrate (DLKTM). This is a hydrate of comparatively high thermal stability (El Saffar & Johnson 1976) and can be prepared as large well-formed crystals that are particularly suitable for kinetic investigations. The relatively low reactivity of DLKTM permits vacuum measurements during the initial stages to be completed more reliably than for many of those previously studied hydrates from which water losses are readily and rapidly initiated at ambient temperature. Our selection of this little studied compound has since developed into a series of complementary and interlinked investigations that have given new insights into diverse aspects of the chemistry of these initially solid reactants.

This two part report (part II is the following paper) is concerned with the dehydration of

$$d\ \mathrm{LiKC_4H_4O_6.H_2O}.$$

Part I describes the initial water evolution rate process during which water loss is restricted to the crystal periphery and is diffusion controlled, some aspects of which were reported previously (Galwey & Okhotnikov 1988). Subsequently, nuclei are developed in or below this layer and the reaction interfaces generated progress thereafter into the reactant as the periphery of the zone of product recrystallization: this process is reported in part II. Thus this reactant exhibits both types of behaviour characteristic of dehydrations.

Other work concerned with these salts shows that dehydration rates vary with anion stereochemistry (*d*, *dl* and *meso* forms of the tartrate anion) in compounds of identical compositions (Baranov *et al.* 1990). Studies of the *dl* (Bhattamisra *et al.* 1992) and *meso* (Galwey *et al.* 1992) $\mathrm{LiKC_4H_4O_6}$ hydrates showed that both salts comprehensively melt during dehydration. This melting has been confirmed by microscopic examinations of partially reacted salt specimens and the kinetic characteristics show (not unexpected) parallels and similarities of behaviour with solid state reactions. We believe that the formulation of a meaningful reaction mechanism for any chemical reaction of a solid requires the positive establishment

of whether or not that reaction proceeds with melting. Throughout our studies in this area, central aims have been to determine the influence of structure on reaction mechanism and the role of melt formation, if any.

A kinetic study of the anion decomposition reactions of the anhydrous lithium potassium tartrates has been reported recently (Galwey & Laverty 1993). These salts also undergo melting during reaction.

2. The early stages of dehydration of crystalline hydrates

General reviews of the earlier literature on this topic have been given by Garner (1955) and by Brown *et al.* (1980). Freund (1968) suggested that in the dissociation,

$$\mathrm{AB(s)} \rightleftharpoons \mathrm{A(s)} + \mathrm{B(g)},$$

a vacant site, A*(s), appears within the solid that initially retains a structure similar to that of the reactant, AB(s). As product formation proceeds the number of vacant sites increases and the vacancy structure develops, usually accompanied by intracrystalline diffusion of B. Subsequently, microcrystals of the thermodynamically stable residual product, A(s), become detached following structural rearrangements induced by high vacancy concentrations within the reacted zone. This model was later developed in articles by Mutin & Watelle-Marion (1972) and by Niepce *et al.* (1973). Vacancy structure development was observed in mechanistic studies of water losses from several hydrates, including $MoO_3.H_2O$ (Oswald *et al.* 1975), $CuSO_4.5H_2O$ (Zagrai *et al.* 1978; Boldyrev *et al.* 1987) $BaC_2O_4.H_2C_2O_4.2H_2O$ (Mutin *et al.* 1979) and also in the decomposition of $NiPt(CN)_4 \cdot 2NH_3$ (Reller 1985).

Studies of alum dehydrations (Galwey *et al.* 1981) and water evolution from other crystalline hydrates (Guarini *et al.* 1983) have concluded that, in vacuum, water losses initially occur across all boundary crystal surfaces. This dehydration is, however, restricted by the inability of the salt to recrystallize, except at specific sites of imperfection wherein the generation of a nucleus is possible. Surfaces, featureless after evacuation, undergo textural modifications that become microscopically visible after alterations that occur on exposure to water vapour. This is identified as water promoted modification of a superficial vacancy structure, previously generated by diffusive removal of water molecules, through water accommodating site vacancies.

The mathematical theory of non-stationary diffusion, applicable to diffusive dehydrations without structural modification, has been discussed by Okhotnikov & Babicheva (1988). They derived the kinetic expression

$$\alpha = At - Bt^{\frac{3}{2}} \qquad (1)$$

for mass losses (proportional to α) during the early stages of dehydration when the diffusion coefficient is approximately constant: α is the fractional reaction at time t and A and B are constants. Equation (1) has been shown to be obeyed satisfactorily during the early stages of $Li_2SO_4.H_2O$ dehydration of single crystals (Okhotnikov *et al.* 1989) and for the dehydration of vermiculite single crystals (Okhotnikov & Babicheva 1988; Okhotnikov *et al.* 1989). The diffusion coefficient for water migration in vermiculite, obtained from equation (1), agreed well with independent data from quasi-elastic neutron scattering measurements (Tuck *et al.* 1985).

The present work reports a detailed study of the kinetics of DLKTM dehydration. It also provides a quantitative theoretical explanation of rate data based on water diffusion within a developing vacancy structure. The extent of the initial deceleratory

stage of this reaction is limited and it is followed by a nucleation and growth reaction that is the subject of Part II (following paper). Complementary studies of both reactions provide evidence that initial limited depth dehydration proceeds on all crystal faces before and during the establishment of growth nuclei (Galwey *et al.* 1981).

3. Experimental

Parallel and complementary dehydration kinetic studies were completed in Novosibirsk (N) and in Belfast (B), using different experimental techniques and different preparations of the same reactant compound: *d* lithium potassium tartrate monohydrate.

(*a*) *Reactant preparations*

Salt A (N)

d-$LiKC_4H_4O_6 . H_2O$ was crystallized from stoichiometric ratios of LiOH, KOH and *d*-$C_4H_6O_6$ is aqueous solution. On slow evaporation at 313 K, single crystals of good optical quality were obtained. Reactant composition determined by combustion analysis (C, 22.68; H, 2.98%) was in good agreement with theoretical expectation (C, 22.65; H, 2.85%). Disc shaped reactant specimens were cut from acceptably perfect crystals, by the technique described previously (Okhotnikov & Lyakhov 1984; Okhotnikov *et al.* 1989), oriented with the flat face parallel to the (001) crystallographic plane. Each sample used for kinetic measurements was washed with a 1:1 ethanol:water mixture to eliminate the possible activation effects from the cutting process: this contrasts with our earlier studies (Galwey & Okhotnikov 1988) which used 'as cut' faces polished with a diamond paste.

Salt B (B)

The same reactant salt was obtained by evaporation of a saturated solution containing stoichiometric proportions of Li_2CO_3, K_2CO_3 and *d*-$C_4H_6O_6$. Again the salt composition, determined by combustion analysis (C, 22.40; H, 2.85%), was in close agreement with the theoretical requirements for *d*-$LiKC_4H_4O_6 . H_2O$. Crystals of size suitable for kinetic studies, 5 mm × 3 mm × 3 mm, were obtained directly from the evaporating basin, sometimes requiring oriented cleavage from larger crystals.

4. Experimental methods

(*a*) *Mass loss measurements* (N)

Dehydration kinetics, for the early stages of reaction, were measured for a 6 mm diameter disc of salt, 1 mm thickness, using a quartz crystal microbalance (Okhotnikov & Lyakhov 1984; Okhotnikov *et al.* 1989). Mass changes were measured with an accuracy $\pm 10^{-8}$ g, temperature was controlled ± 0.1 K and a dynamic vacuum 7×10^{-5} Pa was maintained over the reactant crystal face throughout. Water loss occurred from the single exposed (001) face only; other surfaces were rendered inactive by a covering of indium-gallium eutectic (Galwey & Okhotnikov 1988).

(*b*) *Evolved water vapour pressure measurements* (B)

The kinetics of water evolution were also measured using a conventional glass vacuum apparatus, of known volume and initially evacuated to less than 10^{-2} Pa. After closing the tap to the pumps, the extent of dehydration was determined from the pressure of accumulated water vapour at appropriate times. Pressure values were

measured ± 0.1 Pa in the range 0–1500 Pa and the temperature of the reactant salt was maintained constant ± 0.5 K. Kinetic data (time, temperature, pressure of water vapour) were recorded automatically at prespecified time intervals; the experimental apparatus and method have been described in detail elsewhere (Carr & Galwey 1986).

Experiments were concerned with dehydrations of individual single crystals and also with crushed powders. Both types of reactant were studied from initiation of dehydration in vacuum and also in the presence of a preadmitted known pressure of water vapour.

(*c*) *Electron microscopy* (B)

Kinetic studies were complemented by electron microscopic examinations of salt B crystals after uncompleted reactions to various measured extents. For examination of external faces, specimens were mounted directly and those for examination of internal features were first cleaved to expose the textures of interest. Each specimen was coated lightly with gold before examination in the Jeol 35CF scanning electron microscope. The stability of the reactant was only just sufficient to enable this work to be undertaken. On prolonged observation, sample deterioration became obvious, so that care had to be taken to limit electron beam exposure and magnification before detail was lost. All microscopic work has been completed and interpreted with due regard for the possible occurrence of changes during examinations.

5. Results and discussion

The detailed kinetic and microscopic investigation of the dehydration of *d*-$LiKC_4H_4O_6.H_2O$ has shown that water loss between 400–470 K is completed without comprehensive melting and that two distinct rate processes are involved. The first reaction (with which this paper is exclusively concerned) is identified as a deceleratory, diffusion-controlled release of water from a superficial reactant layer of thickness *ca.* 10 μm. This represents a small proportion of the total reaction for single crystals (*ca.* 5%) and a relatively greater proportion for crushed powder (up to 50%) where the effective surface area of the reactant is much larger. The second reaction (described in part II) is initiated towards completion of the first and the extent of overlap is small. This is a nucleation and growth process, confirmed by microscopic observational evidence. No significant kinetic interdependence of the two reactions was detected and these were, therefore, analysed as separate and distinct rate processes. Anion breakdown was separately studied in a temperature interval (greater than about 490 K) appreciably above the range of the present dehydration investigations (Galwey & Laverty 1993).

(*a*) *First reaction: mass-loss measurements*

Typical mass-loss–time curves for the early stages of the isothermal dehydration from the exposed flat surface of the disc-shaped single crystal specimens of DLKTM, salt A, are shown in figure 1*a–c*. The form of the deceleratory behaviour observed is characteristic of rate control by diffusion from a semi-infinite medium. Our kinetic analysis considers, therefore, the description of these data by equation (1), most conveniently compared in the differential form (Okhotnikov *et al.* 1989)

$$\begin{aligned}(\mathrm{d}m/\mathrm{d}t) &= \rho Sk - (2\rho Sk^2/\pi^{\frac{1}{2}}D_0^{\frac{1}{2}})\,t^{\frac{1}{2}} \\ &= A_0 - \tfrac{3}{2}B_0\,t^{\frac{1}{2}}, \end{aligned} \qquad (2)$$

where ρ is the density of water in the crystal (0.137 g cm^{-3}), S is the reactant surface

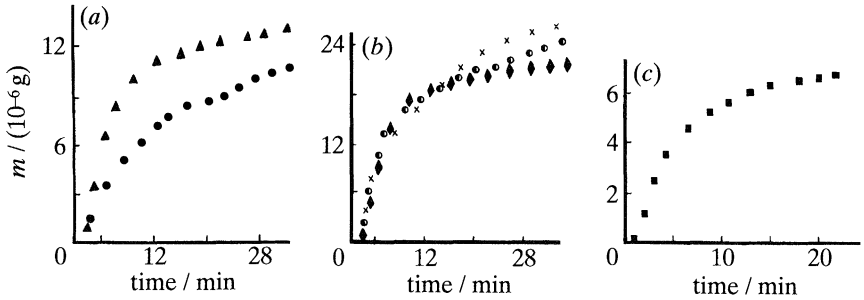

Figure 1. Initial stages of the weight loss (m) against time plots for the dehydration of DLKTM single crystal (001) faces in vacuum (6.7×10^{-5} Pa) at the following temperatures. (a) ●, 363 K; ▲, 380 K. (b) ◆, 395 K; ○, 403 K; ×, 414 K. (c) ■, 423 K.

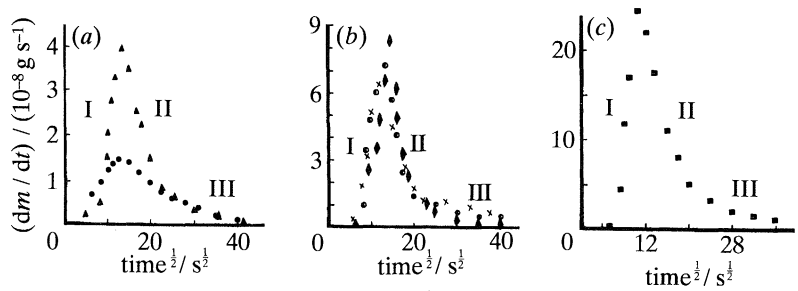

Figure 2. Plots of rate of mass loss ($\mathrm{d}m/\mathrm{d}t$) against $t^{\frac{1}{2}}$ for data in figure 1. The significance of regions I, II and III is discussed in the text. (Symbols as in figure 1.)

Table 1. *Diffusion coefficients for the dehydration of d-lithium potassium tartrate monohydrate single crystal (001) faces at several temperatures*

temperature/K	$k/(10^{-6}$ mm s$^{-1})$	$D_0/(10^{-8}$ mm^2 s$^{-1})$	$D_{\mathrm{eff}}/(10^{-10}$ mm^2 s$^{-1})$
363	5.09±0.08	1.42±0.09	20.13±0.08
380	13.9±0.2	4.13±0.05	5.55±0.07
395	30.8±0.7	10.0±0.2	10.88±0.03
403	22.1±0.6	7.57±0.06	24.6±0.1
414	24.5±0.5	9.61±0.08	52.6±0.6
423	92.0±1.0	121.0±0.1	393±3

area (28 mm^2), t is time, ($\mathrm{d}m/\mathrm{d}t$) is the rate of mass loss, k is the rate constant for transition of water molecules from the chemically bonded to the free state, D_0 is the diffusion coefficient for water in the crystal structure and A_0 and B_0 are constants. This test of description of the data in figure 1 by equation (2) is shown as plots of ($\mathrm{d}m/\mathrm{d}t$) against $t^{\frac{1}{2}}$ in figure 2. Three distinct water evolution rate processes can be recognized; these are labelled on the figure 2*a–c*.

Region I extends to the maximum of the differential plot. The amount of water lost, $\alpha \approx 0.001$, was the same for all samples and was independent of temperature. This is identified, therefore, as the release of physically adsorbed, superficial water including that within cracks and pores and retained by the solution-grown crystals.

Region II is the deceleratory phase of water evolution and is satisfactorily expressed by equation (2). Values of k and D_0, calculated by the method of least squares from our data, are reported in table 1. Water losses from the crystal, following outward diffusion, result in the generation of increasing concentrations of

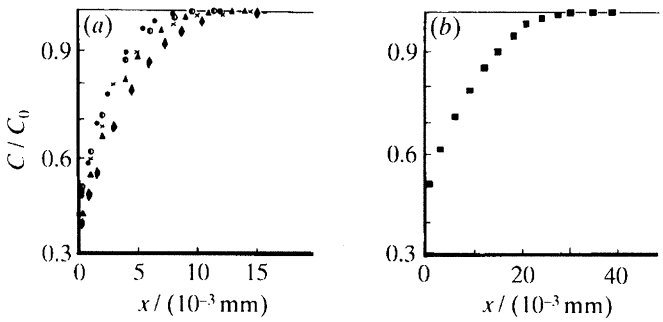

Figure 3. Plots of variation in water molecule concentration (C/C_0) with distance inward from crystal face at the time of transition from region II to region III calculated from data in figures 1 and 2, using equation (3) in text. (Symbols as in figure 1.)

vacancies at water-accommodating lattice sites within the zone from which this loss has occurred. This results in two competing effects. (i) There is a progressive increase in the elastic strain energy (Galwey & Guarini 1978) which may lead to cracking. (ii) Modification of the vacancy structure through thermally induced movements of the other crystal components may cause changes in the diffusion permeability of the vacancy structure for water. From the results in figure 2, it is apparent that a point is reached at which the flow of molecular water, measured as ($\mathrm{d}m/\mathrm{d}t$), reaches a plateau value recognized as the transition to the subsequent slow process, *region III*.

Profiles of the concentration of water molecules in the vicinity of the crystal surface can be calculated, by the theory of diffusion, using (Krank 1975)

$$\frac{C(x,t)}{C_0} = \mathrm{erf}\left(\frac{x}{2D_0^{\frac{1}{2}}t^{\frac{1}{2}}}\right) + \exp\left(\frac{kx}{D_0} + \frac{k^2t}{D_0}\right)\mathrm{erfc}\left(\frac{x}{2D_0^{\frac{1}{2}}t^{\frac{1}{2}}} + \frac{kt^{\frac{1}{2}}}{D_0^{\frac{1}{2}}}\right), \tag{3}$$

where $C(x,t)$ is the concentration of water molecules at time t and distance x below the surface. Calculated water molecule concentration profiles, represented inward from the crystal face and corresponding to the time of transition of region II to region III (see figure 2) are shown in figure 3, using k and D_0 values from table 1. These concentration profiles, $C(x,t)/C_0$, are almost independent of temperature.

Data in region II, figure 2, may be described by equation (2) and physically this represents the combination of the two processes described by k and D_0. However, after the diffusion controlled distribution of vacancies becomes distorted through structural change, mass transfer becomes controlled by diffusion only and fits the expression (Okhotnikov *et al.* 1989)

$$m(t) = -\frac{\rho S D_{\mathrm{eff}}}{k_{\mathrm{eff}}} + \frac{2\rho S D_{\mathrm{eff}}^{\frac{1}{2}}}{\pi^{\frac{1}{2}}}t^{\frac{1}{2}}. \tag{4}$$

Numerical values for the effective diffusion coefficient D_{eff}, calculated for region III, using plots of m against $t^{\frac{1}{2}}$, figure 4, and the least square method are given in table 1. Values of D_0 and D_{eff} differ by about two orders of magnitude: this is in good agreement with the experimental results that show that the diffusional flux of water decreases abruptly at the transition from region II to region III.

Diffusion coefficient values reported by Galwey & Okhotnikov (1988), using similarly measured data, were calculated from

$$m^2 = (\rho S)^2\pi^{-1}Dt, \tag{5}$$

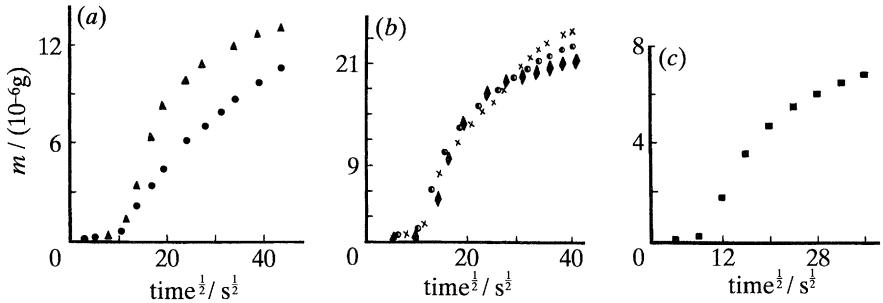

Figure 4. Plots of m against $t^{\frac{1}{2}}$, for data from figure 1, to test obedience of one-dimensional diffusion model (equation (4)). Values of D_{eff} have been calculated for the latter part of reaction, region III. (Symbols as in figure 1.)

which assumes a solid–solid interface. The recognition that rate behaviour is more realistically represented by loss from the solid–gas interface gives a different value for the effective diffusion coefficient: $D_{\text{eff}} = 0.25D$ (see Okhotnikov *et al.* 1989).

(*b*) *Scanning electron microscopic studies*

Previous electron microscopic studies (Galwey & Okhotnikov 1988) have shown that surfaces of DLKTM crystals underwent considerable textural changes before the appearance of dehydration nuclei. These are identified as structural reorganizations within a thin superficial layer of the crystal and are to be distinguished from melting in that there have been limited bond redistributions within the outer layer of distorted, or possibly vitreous, material. The extensive hydrogen bonding in the salt is expected to enhance the stability and diversity of local packing arrangements to form an irregular structure that may be regarded as a vitreous phase. This reorganization is conveniently termed *vacliquescence* to emphasize the role of vacancy accumulation at water sites in generating stress that is relieved by bond redistributions within the reactant. Lattice order is thereby reduced and a more stable but less regular structure is achieved without fusion.

Single crystals

Characterization of the textural changes occurring during the diffusion controlled first reaction was based on observations using large single crystals of salt B. α values mentioned refer to the completed reaction. Dehydrated product crystals ($\alpha = 1.00$) were pseudomorphic with those of the reactant. There was no evidence that the reactant underwent comprehensive melting, though crushed powder particles aggregated by sintering during dehydration.

Partly dehydrated crystals characteristically exhibited a textural transformation within the outer 1 μm superficial layer; a typical restructured superficial zone, in section, is shown in figure 5 ($\alpha = 0.15$ at 433 K). This readily distinguished feature was observed for all faces of partly reacted material; modified layers were always of similar thickness (*ca.* 1 μm) and strongly adhered to the crystal. This thickness was much less than that required to account for the total water yield from the first reaction. From the calculated distribution curve for residual water molecules, figure 3, we estimate that the phase discontinuity is developed at $C(x,t)/C_0 \approx 0.6$ and structural reorganization occurs when this value is exceeded. The modified outer surface layer is believed to possess some fluid characteristics at reaction temperature

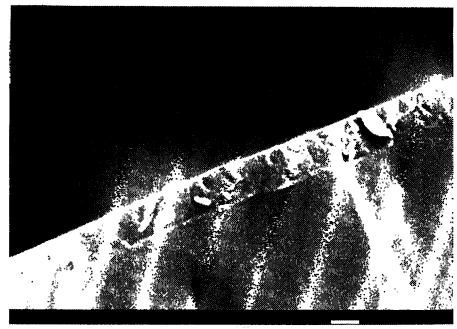

Figure 5. Scanning electron micrograph of a section of a partly dehydrated DLKTM single crystal ($\alpha = 0.15$ at 433 K). A superficial outer layer of reorganized material, thickness *ca.* 1.0 μm, is clearly revealed. Scale bar: 1.0 μm.

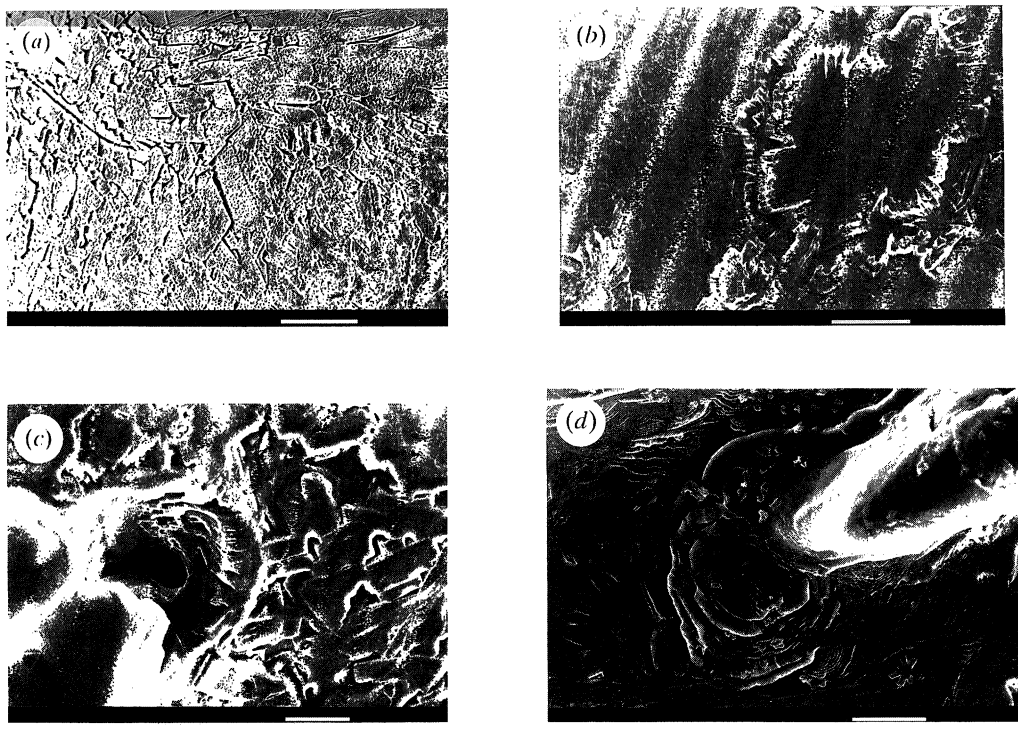

Figure 6. Representative scanning electron micrographs showing surface textures developed after dehydration of DLKTM crystals. All scale bars: 10 μm. (*a*) Relatively planar, but extensively fissured and pitted surface of a fully dehydrated crystal ($\alpha = 1.00$ at 433 K). (*b*) Evidence of local superficial recrystallization of surface of a partially dehydrated crystal ($\alpha = 0.12$ at 433 K). (*c*) and (*d*) Zones of local surface modification associated with subsurface evolution of water during the second rate process. These two areas of the same crystal face show (*c*) a pore and (*d*) evidence of interrupted flow associated with repeated bubble formation ($\alpha = 0.12$ at 420 K).

because features tend to be rounded, as if subject to surface tension control (figure 6*a*) and can further modify on cooling in a locally irregular recrystallization process (figure 6*b*). More direct evidence of the flow characteristics of this outer layer is seen in figure 6*c*, *d*, where the circular and concentric patterns are ascribed to sub-surface

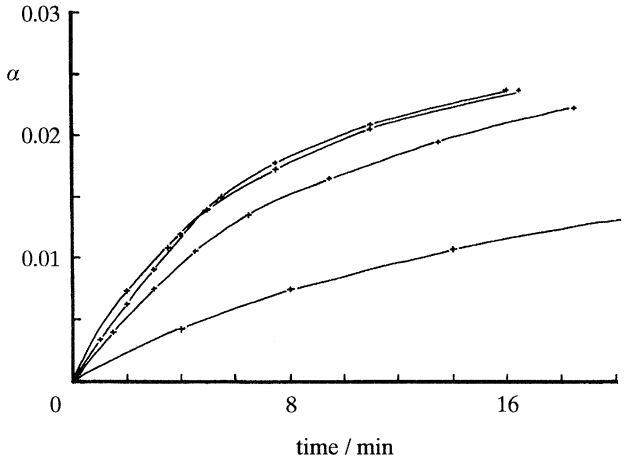

Figure 7. Plots of α against time for the first reaction in the isothermal dehydration of DLKTM single crystals at 422.5 K. (α values calculated for completed salt dehydration.)

water evolution during the second reaction. Water evolved below the boundary layer escapes by bubble formation (part II) and the patterns seen indicate that the textures, generated by intermittent gas escape through a viscous fluid, forming holes and concentric rounded ripple-like features, are retained after cooling.

From this evidence, we conclude that the extensively dehydrated (more than 40%) outer crystal layer is transformed from the monohydrate crystal structure to a highly viscous liquid or a vitreous phase. The modified zone remains strongly attached to the related subsurface hydrate but, where water is expelled (locally, during the second reaction), some may be reaccommodated within the outer layer, so decreasing viscosity and thereby achieving liquid properties.

(c) *First reaction: water vapour pressure measurements*

Single crystals, salt B

Typical plots of α against t for the deceleratory first reaction of salt B single crystals at 422.5 K are shown in figure 7. α values were calculated from pressure measurements based on the completed reaction and complement the gravimetric studies described above. The first reaction was completed at $\alpha = 0.03$–0.04 for crystals of edges 2–3 mm, mass 40–50 mg and surface areas 50–60 mm^2.

Comparisons between the pressure and the gravimetric data must include consideration of the differences inherent in the alternative experimental techniques used. Single crystal dehydration (salt B) was possible from all faces, solution grown and cleaved, in contrast with studies of salt A concerned exclusively with water losses from the prepared (001) faces. Each crystal of salt B required 4–5 min to achieve reaction temperature in the vacuum apparatus, consequently regions I and II, completed within *ca.* 5 min at 423 K (figure 2*c*), could not be investigated. Accordingly, these water evolution measurements were concerned with region III only, the diffusion-controlled process.

Water evolution data obeyed equation (4). Plots of p^2 (water vapour pressure evolved is directly proportional to m) against t were invariably linear in all our measurements; two typical examples are shown in figure 8. The positive intercept on the time axis represents the delay in attaining reaction temperature, together with

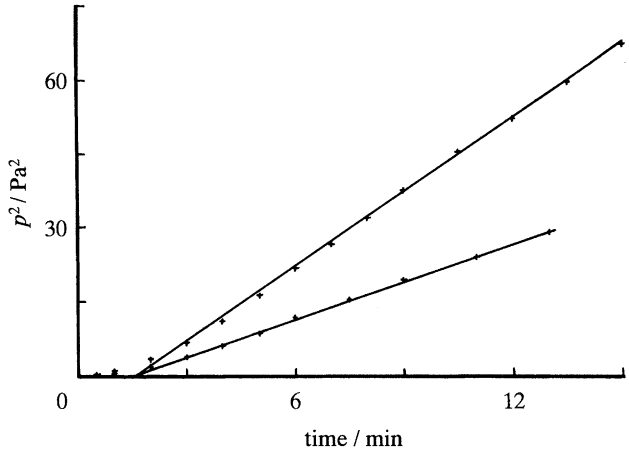

Figure 8. Linear plots of (water vapour pressure)^2 against time for the initial stages of isothermal dehydration of DLKTM single crystals at 422.5 K, showing obedience to equation (4).

contributions from the initial processes, regions I and II. Of greater theoretical significance here, however, are the marked variations in rate coefficients for dehydrations of successive, apparently identical, crystals. Such variations were generally characteristic of this process and are clearly evident in figure 8. This irreproducibility is ascribed to differences in imperfection concentrations and distributions for the individual crystals because such zones of structural distortion provide the pathways through which water escape preferentially proceeds. Imperfection structures are sensitive to crystal preparation conditions. The individual strain pattern developed in each crystal during dehydration is determined by the local defect distribution that controls the water site vacancy concentration profile and consequently the rate of water release. Further factors that contribute to rate variations are the differences in individual crystal surface areas, surface roughness, surface damage and the relative perfection of the boundary layers. Rate constants for water diffusion at 422 K varied in the range 12.6 ± 7.6 Pa^2 s^{-1}, a considerably greater scatter of values than that characteristic of reactant surfaces (salt A, Galwey & Okhotnikov 1988) which had been prehomogenized by abrasion with diamond paste.

All results for the first reaction are compared in the Arrhenius plot, figure 9. These results demonstrate convincingly that identical controls operate under both conditions. The diffusion parameters for this rate process, subject to the recalculation mentioned above, are activation energy for diffusion, $E_D = 153 \pm 4$ kJ mol^{-1} and $D_{\text{eff}} = 7.5 \times 10^6$ mm^2 s^{-1}. There was no evidence that during reaction the accumulated evolved water vapour significantly influenced the dehydration kinetics.

Crushed crystals, salt B

Dehydrations of crushed crystals result in a much more extensive first reaction than that for large crystals, almost half of the constituent water is evolved. This is ascribed to the large increase in surface area following crystal disintegration. Approximate calculations confirm that the thickness of the vacancy structure layer on completion of this initial process corresponded to the dehydration of a superficial crystal layer of 8–10 μm, similar to that found for single crystals. This rate process is deceleratory, figure 10 (compare with figure 7 for crystals also at 422 K). Again

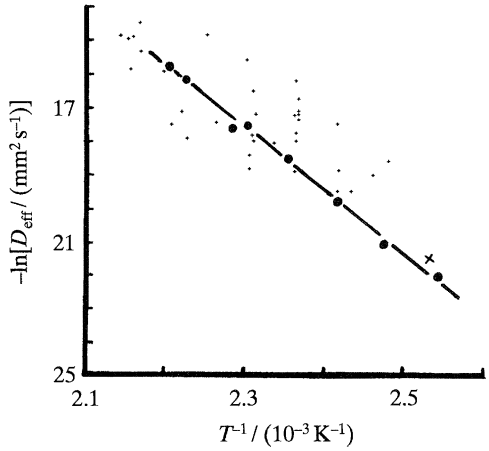

Figure 9. Arrhenius plots for diffusion coefficients, D_{eff}, for the initial rate process during dehydration of DLKTM single crystals between 400–460 K. The considerable scatter of values for individual untreated crystals is attributed to control of reaction rate by imperfection structure. These data are scattered about the line (●) measured in earlier studies (Galwey & Okhotnikov 1988) using cut and polished prepared surfaces. The mean value (×) of four points from a further study has also been included.

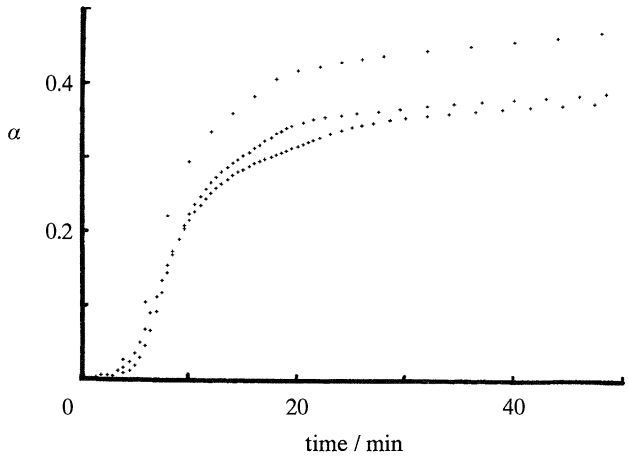

Figure 10. Plots of α against time for the first reaction during dehydration of DLKTM crushed powder at 422.5 K.

kinetic data, after a warm-up period of 4–5 min, were described by equation (4), see figure 11, behaviour identical with the diffusion controlled first reaction of single crystals. Diffusion coefficients, calculated from measurements between 390–472 K, were all close to data for dehydration from (001) crystal faces, as shown by the comparison on the Arrhenius plot, figure 12. The scatter of measured values was significantly less than that calculated for single crystals of salt B (figure 9). These variations include some uncertainty in surface area measurements but were more probably a consequence of the achievement of an average crystal imperfection distribution, in the mechanically disintegrated salt. Crushing may be expected to remove gross imperfections, invariably sites of crack initiation. Cold working will presumably modify crystallite surfaces to generate comparable distributions and concentrations of structured defects. The average surface textures, generated on

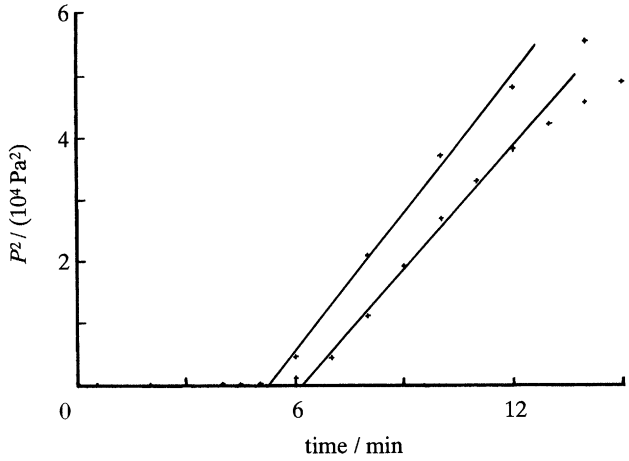

Figure 11. Linear plots of (water vapour pressure)^2 against time for the early stages of the first reaction of DLKTM crushed powder at 422.5 K: equation (4) is obeyed.

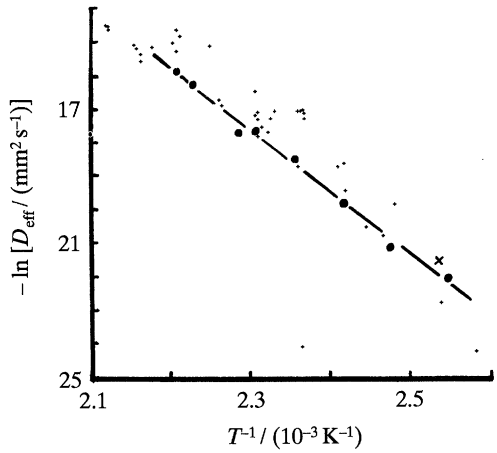

Figure 12. Arrhenius plots for diffusion coefficients D_{eff} calculated for the first reaction of DLKTM crushed powder 390–472 K. Data are again close to the line for the cut and polished surface (the line and points here are the same as those shown on figure 9).

crushing, will constitute the greater proportion of powder surfaces and this contrasts with the possibly atypical boundaries developed during crystal growth and subsequent drying after removal from solution.

X-ray diffraction patterns for salt B, crushed and partly dehydrated to known extents, showed no change of crystal structure when $\alpha < 0.23$. This is consistent with the suggested mechanism that water loss generates a vacancy structure, which must be extensive before recrystallization occurs.

(*d*) *Influence of water vapour pressure on first reaction*

Reactions were initiated in various pressures of water vapour present in the apparatus before kinetic studies. All reactions hotter than 420 K and pressure less than 1.2×10^3 Pa (H_2O) proceeded to complete evolution of the constituent water of the monohydrate (i.e. $\alpha = 1.00$). There was no evidence in any experiment that equilibrium was reached between water in the crystal and that in the vapour phase.

Table 2. *Diffusion coefficients for the dehydration of d-lithium potassium tartrate monohydrate single crystals and powder at 423 ∓ 1 K for reaction initiated in various initial water vapour pressures*

single crystal									
initial water vapour pressure/Pa	0	120	350	430	640	660	840	930	1120
$D_{eff}/(10^{-7}\ mm^2\ s^{-1})$	1.54	1.82	11.0	3.5	5.0	33.7	30.25	16.35	125
crushed crystal									
initial water vapour pressure/Pa	0	130	500	640	680				
$D_{eff}/(10^{-7}\ mm^2\ s^{-1})$	0.250	0.035	0.0625	0.0225	0.050				

Single crystals

At low pressures of preadmitted water vapour (less than 650 Pa) the rate of the first reaction at 423 K was appreciably increased and the extent was increased slightly to $\alpha = 0.045 \pm 0.010$. Data for single crystals (*ca.* 45 mg) are reported in table 2. This behaviour is explained by the development of vacancy structures during initial water loss (region II) during which the flux of water molecules is expressed by

$$\frac{\partial C}{\partial t} = \frac{\partial}{\partial x}[D(C).\partial C/\partial x], \tag{6}$$

where $D(C)$ is the concentration dependent diffusion coefficient and $(\partial C/\partial x)$ is the concentration gradient (Okhotnikov *et al.* 1989).

During the vacuum dehydration of the present reactant, $\partial C/\partial x$ is large and the flux is also expected to be large. This initial rapid water loss creates many sub-surface water site vacancies in which the disordered structure inhibits further loss from the underlying crystal bulk (i.e. $D(C)$ is small). Thus the initial dehydration effectively becomes self-inhibiting. When water vapour is present at the onset of reaction, the initial subsurface water concentration gradient generated $(\partial C/\partial x)$ is relatively reduced, the rate of water loss is diminished but the water site vacancy structure is less distorted, thus permitting the first reaction to proceed further.

Dehydration measurements for reactions initiated in higher pressures of preadmitted water required the use of smaller reactant masses (*ca.* 10 mg crystal) with a consequent reduction in experimental accuracy. The extents of the first reaction systematically rose with pressure from $\alpha = 0.15$ to $\alpha = 0.28$ in 650–1200 Pa (H_2O): see figure 13 and table 2. Diffusion coefficients were increased by a factor of about 20, though no systematic trends were identified. This behaviour pattern is entirely consistent with the theoretical considerations discussed in the previous paragraph.

Studies of the dehydration kinetics of the layered mineral vermiculite (Mikhail *et al.* 1970) showed a similar pattern of dependence of reaction rate on prevailing water vapour pressure. Water losses in water vapour proceeded more rapidly than the reaction in vacuum, ascribed to the retention of a proportion of the interlayer water thus stabilizing the interlayer spacing and facilitating diffusive loss of H_2O molecules.

Crushed powder

Representative α-time plots for the first reaction of salt B at 423 K in 0–680 Pa (H_2O) are shown in figure 14. Values of D_{eff} calculated from these data are given in table 2 and show that there is a significant reduction in dehydration rate

PHILOSOPHICAL TRANSACTIONS OF THE ROYAL SOCIETY A MATHEMATICAL, PHYSICAL & ENGINEERING SCIENCES

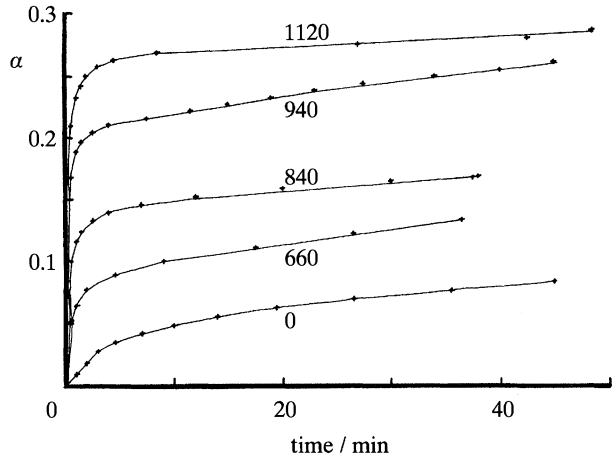

Figure 13. Plots of α against time for the first reaction during dehydration of DLKTM single crystals at 423 K initiated in the various water vapour pressures specified (Pa).

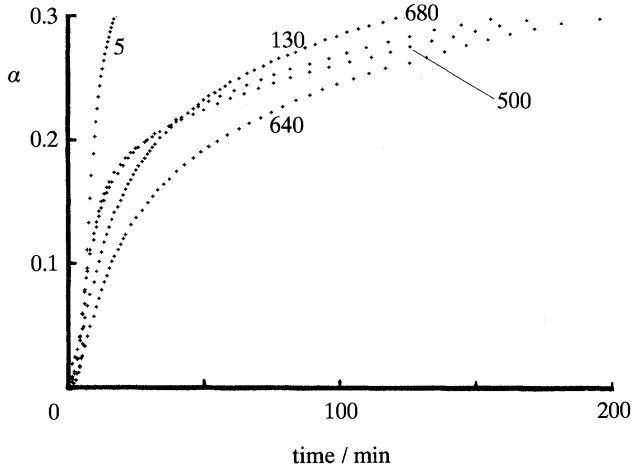

Figure 14. Plots of α against time for the first reaction during dehydration of DLKTM crushed powder at 423 K initiated in the various water vapour pressures specified (Pa).

$\times (0.17 \pm 0.07)$ when preadmitted water is present. Values (table 2) show some scatter but there is no significant change in magnitude with increase in water vapour present before onset of reaction. This rate diminution is ascribed to the water vapour adsorbed on the external crystallite faces so that the consequent surface modification reduces the ease of water loss. Crystal crushing is expected to destroy the zones of maximum imperfection and result in a generally more homogeneous boundary layer structure. Sintering and crystallite aggregation during reaction are also known to reduce somewhat the effective surface area from which water is lost.

6. Conclusions

This study confirms and provides considerably extended experimental and theoretical foundations for the previously expressed view (Galwey *et al.* 1981) that the dehydration of a crystalline hydrate may initially occur across all surfaces but to a limited depth. In some crystalline ionic hydrates, the subsequent second reaction

may proceed by an alternative mechanism involving the development and growth of nuclei (Brown *et al.* 1980); the role of interface reactions in the continued dehydration of DLKTM is discussed in part II. This paper is exclusively concerned with the first reaction, a dehydration process that has not previously been subjected to such detailed scrutiny. This was possible because of the considerable thermal stability of the hydrate, from which all of the water of crystallization from the monohydrate was evolved in a single temperature range, albeit by two rate processes.

Processes contributing to the first reaction were investigated gravimetrically for (001) crystal faces, in which the following stages were distinguished (figure 2).

Initially (region I) there was a rapid release of a small amount of water ($\alpha = 0.001$) that was loosely bonded or in stoichiometric excess at or near the crystal face.

Subsequently, the rate of water evolution progressively diminished by a process (region II) identified as being controlled by H_2O diffusion within a developing vacancy structure at water-accommodating sites located in the zone immediately beneath the crystal surface. During this rate process the original structure of the salt was largely maintained.

Thereafter (region III) water loss continued by H_2O migration within an increasingly disordered vacancy structure. The diffusion coefficient was sensitive to the original defect structure of the crystal and the extent of water loss.

Water released during these three stages corresponded to the complete dehydration of a superficial crystal layer of thickness 10 μm. Microscopic examinations of sections revealed a pronounced textural change at 1 μm (figure 5), corresponding to the zone from which water loss exceeded 40%. Although sought, there was no evidence of any textural modifications within the zone beneath the 1 μm discontinuity, from which water losses had undoubtably occurred.

Single crystal measurements gave evidence that reactivity at different crystallographic faces was similar but the significant reactivity variations between individual crystals was ascribed to changes in the local concentrations, distributions and types of imperfections present. Such variations were less for powdered reactants, from which we conclude that cold working during crushing generates a larger surface but that the overall average reactivity is more nearly constant.

Dehydrations of single crystals increased in both rate and extent when water vapour was present prior to onset of reaction. From the theory of intracrystalline diffusion it is concluded that the water-site vacancy distribution, within the superficial zone from which water has been lost, is modified resulting in the observed (figure 13 and table 2) increase in reaction rate constant and the depth from which water is released (regions II and III). Textural features, developed at crystal surfaces during the second reaction (figure 6*c*, *d*), provide evidence that at sites of continued water release there is viscous flow of the surface layer. This results, perhaps, from temporary reaccommodation of water in dehydrated salt during emission from reaction in the crystal interior.

In contrast, during the reaction of crushed powder samples such liquefaction or reduction in the viscosity of a surface layer, by accommodation of excess water vapour present, may enhance crystallite sintering. Such aggregation of particles must lead to a diminution of the area of surface from which water is lost and explains the reductions in rate and extent of water losses (figure 14 and table 2).

This study has shown that this first reaction generates a well-defined superficial zone of extensively dehydrated salt. Kinetic characteristics of this water loss

provides evidence of control through diffusion within a developing vacancy structure (region II) that later becomes disorganized (region III). There was no evidence of recrystallization during the first reaction and it seems probable that the outermost layer may be disordered as in a vitreous phase. Subsequently, the onset of the nucleation and growth (second) reaction is identified with recrystallization and the establishment of a reaction interface that advances into the hydrated reactant.

This model shows features similar to the behaviour previously described for alum dehydrations (Galwey *et al.* 1981). The surface phase described above is, however, very much more extensive than may be generated in the other reactions referred to in the introduction. For the salt, the time and extent of reaction before structural reorganization to the product phase is considerable. Behaviour contrasts with the *meso* and *dl* salts which melt during dehydration (Galwey *et al.* 1992; Bhattamisra *et al.* 1992). The kinetics and mechanism of the second reaction are reported and discussed in part II.

We thank Mr J. McCrae and the Staff of the Electron Microscope Unit of The Queen's University of Belfast for help and advice in obtaining the electron micrographs. G.M.L. thanks the Department of Education for Northern Ireland for the award of a Postgraduate Scholarship held during the time that this work was completed.

References

Baranov, N. A., Okhotnikov, V. B., Rynskaya, L. I., Semenov, A. R., Galwey, A. K. & Laverty, G. M. 1990 *Solid State Ionics* **43**, 37.

Bhattamisra, S. D., Laverty, G. M., Baranov, N. A., Okhotnikov, V. B. & Galwey, A. K. 1992 *Phil. Trans. R. Soc. Lond.* A **341**, 479.

Boldyrev, V. V., Gaponov, Y. A., Lyakhov, N. Z., Politov, A. A., Tolchko, B. P., Shakhtshneider, T. P. & Sheromov, M. A. 1987 *Nucl. Inst. Methods Phys. Res.* A **261**, 192.

Brown, M. E., Dollimore, D. & Galwey, A. K. 1980 *Comprehensive chemical kinetics*, vol. 22. Amsterdam: Elsevier.

Carr, N. J. & Galwey, A. K. 1986 *Proc. R. Soc. Lond.* A **404**, 101.

Cooper, J. A. & Garner, W. E 1940 *Proc. R. Soc. Lond.* A **174**, 487.

Krank, J. 1979 *The mathematics of diffusion*, p. 36. Oxford: Clarendon Press.

El Saffar, Z. M. & Johnson, S. 1976 *J. Chem. Phys.* **64**, 2693.

Freund, F. 1968 *Fortsch. Chem. Forsch.* **10**, 347.

Galwey, A. K. & Guarini, G. G. T. 1978 *J. chem. Soc. chem. Commun.*, p. 273.

Galwey, A. K., Koga, N. & Tanaka, H. 1990 *J. chem. Soc. Faraday Trans. I* **86**, 531.

Galwey, A. K. & Laverty, G. M. 1990 *Solid State Ionics* **38**, 155.

Galwey, A. K. & Laverty, G. M. 1993 *Proc. R. Soc. Lond.* A **440**, 77.

Galwey, A. K., Laverty, G. M., Okhotnikov, V. B. & O'Neill, J. 1992 *J. Thermal Analysis* **38**, 421.

Galwey, A. K. & Okhotnikov, V. B. 1988 *J. Thermal Analysis* **33**, 441.

Galwey, A. K., Spinicci, R. & Guarini, G. G. T. 1981 *Proc. R. Soc. Lond.* A **378**, 477.

Garner, W. E. 1955 *Chemistry of the solid state* (ed. W. E. Garner), ch. 8. London: Butterworth.

Garner, W. E. & Tanner, M. G. 1930 *J. chem. Soc.*, p. 47.

Guarini, G. G. T. & Dei, L. 1983 *J. chem. Soc. Faraday Trans. I* **79**, 1599.

Mikhail, R. Sh., Guindy, N. M. & Hanafi, S. 1970 *J. appl. Chem.* **20**, 34.

Mutin, J. C. & Watelle-Marion, G. 1972 *Bull. Soc. Chim. Fr.* **12**, 4488.

Mutin, J. C., Watelle-Marion, G. & Dusausoy, Y. 1979 *J. Solid State Chem.* **27**, 407.

Niepce, J. C., Dumas, P. & Watelle, G. 1973 Fine particles. In *Proc. 2nd Int. Conf. Electrochem. Soc.*, p. 256. Boston.

Okhotnikov, V. B. & Babicheva, I. P. 1988 *React. Kinet. Catal. Lett.* **37**, 417.

PHILOSOPHICAL TRANSACTIONS OF THE ROYAL SOCIETY A MATHEMATICAL, PHYSICAL & ENGINEERING SCIENCES

Okhotnikov, V. B., Babicheva, I. P., Musicantov, A. V. & Aleksandrova, T. N. 1989 *React. Solids* **7**, 273.

Okhotnikov, V. B. & Lyakhov, N. Z. 1984 *J. Solid State Chem.* **53**, 161.

Okhotnikov, V. B., Petrov, S. E., Yakobson, B. I. & Lyakhov, N. Z. 1987 *React. Solids* **2**, 259.

Okhotnikov, V. B., Simakova, N. A. & Kidyarov, B. I. 1989 *React. Kinet. Catal. Lett.* **39**, 345.

Oswald, H. R., Günter, J. R. & Dubler, E. 1975 *J. Solid State Chem.* **13**, 330.

Reller, A. 1985 Reaction solids. In *Proc. 10th Int. Conf.*, Dijon, p. 869. Amsterdam: Elsevier.

Tuck, J. J., Hall, P. L., Hayes, H. B., Ross, D. K. & Haytes, J. B. 1985 *J. chem. Soc. Faraday Trans. I* **81**, 833.

Zagrai, A. I., Zyryanov, V. V., Lyakhov, N. Z., Chupakhin, A. P. & Boldyrev, V. V. 1978 *Dokl. Akad. nauk. SSSR* **239**, 872.

Received 4 November 1992; accepted 5 February 1993

PHILOSOPHICAL TRANSACTIONS OF THE ROYAL SOCIETY A MATHEMATICAL, PHYSICAL & ENGINEERING SCIENCES

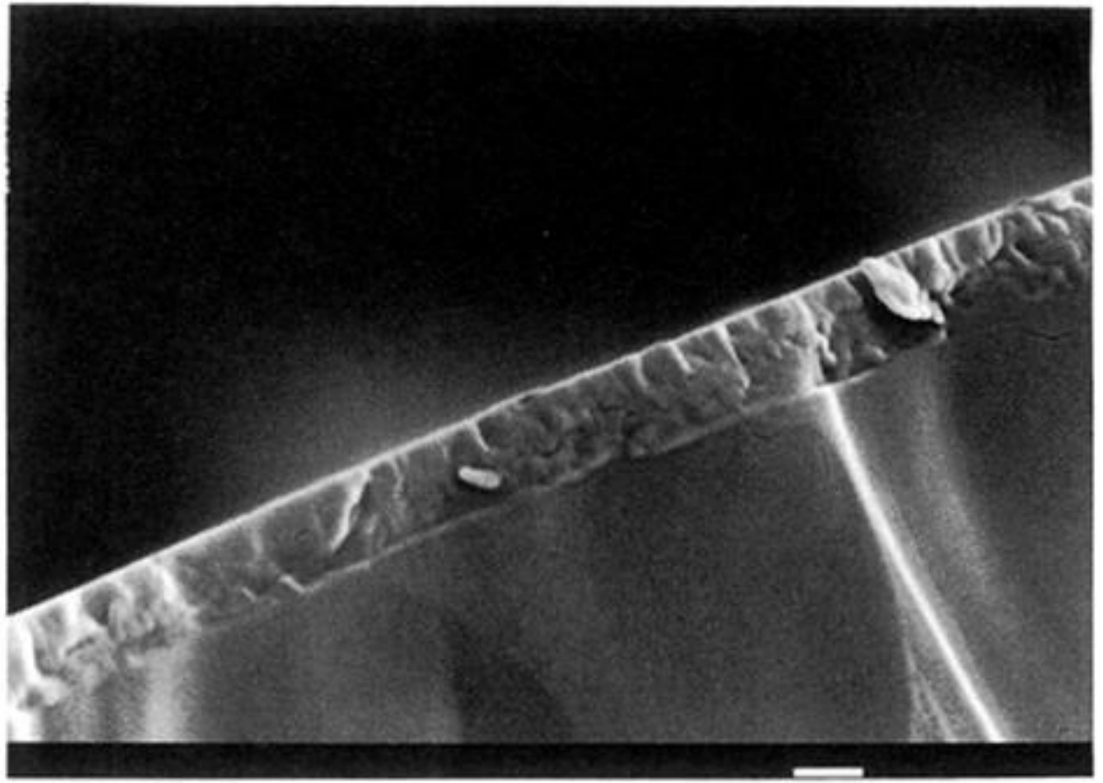

igure 5. Scanning electron micrograph of a section of a partly dehydrated DLKTM single crystal
$\alpha = 0.15$ at 433 K). A superficial outer layer of reorganized material, thickness *ca.* 1.0 μm, is
learly revealed. Scale bar: 1.0 μm.

PHILOSOPHICAL TRANSACTIONS OF THE ROYAL SOCIETY A MATHEMATICAL, PHYSICAL & ENGINEERING SCIENCES

Figure 6. Representative scanning electron micrographs showing surface textures developed after dehydration of DLKTM crystals. All scale bars: 10 μm. (*a*) Relatively planar, but extensively fissured and pitted surface of a fully dehydrated crystal ($\alpha = 1.00$ at 433 K). (*b*) Evidence of local superficial recrystallization of surface of a partially dehydrated crystal ($\alpha = 0.12$ at 433 K). (*c*) and (*d*) Zones of local surface modification associated with subsurface evolution of water during the second rate process. These two areas of the same crystal face show (*c*) a pore and (*d*) evidence of interrupted flow associated with repeated bubble formation ($\alpha = 0.12$ at 420 K).